

MedChemComm

Accepted Manuscript



This is an *Accepted Manuscript*, which has been through the Royal Society of Chemistry peer review process and has been accepted for publication.

Accepted Manuscripts are published online shortly after acceptance, before technical editing, formatting and proof reading. Using this free service, authors can make their results available to the community, in citable form, before we publish the edited article. We will replace this *Accepted Manuscript* with the edited and formatted *Advance Article* as soon as it is available.

You can find more information about *Accepted Manuscripts* in the [Information for Authors](#).

Please note that technical editing may introduce minor changes to the text and/or graphics, which may alter content. The journal's standard [Terms & Conditions](#) and the [Ethical guidelines](#) still apply. In no event shall the Royal Society of Chemistry be held responsible for any errors or omissions in this *Accepted Manuscript* or any consequences arising from the use of any information it contains.

ARTICLE

Exploring cinnamic acid scaffold: development of promising neuroprotective lipophilic antioxidants

Cite this: DOI: 10.1039/x0xx00000x

Daniel Chavarria,^{a,‡} Tiago Silva,^{a,‡} Daniel Martins,^a Joana Bravo,^b Teresa Summavielle,^b Jorge Garrido^c and Fernanda Borges^{a†}Received 00th January 2012,
Accepted 00th January 2012

DOI: 10.1039/x0xx00000x

www.rsc.org/

New lipophilic hydroxycinnamic acid based derivatives were designed, synthesized and their antioxidant and neuroprotective activities evaluated. The chemical modification introduced in the cinnamic acid scaffold lead to compounds' with an amplified lipophilicity and in general with increased antioxidant activity when compared to natural models (caffeic and ferulic acids). The compounds did not display cytotoxicity and present a significant neuroprotective effect against 6-OH-DA induced damage in SH-SY5Y cells. Compound **6** stands out as an efficient radical scavenger and iron (II) chelator that ensures drug-like properties. Moreover, neuroprotection against oxidative damage was observed even at low concentrations (1 μ M). Therefore, compound **6** developed by biology-oriented approach combines important features for a further optimization process that will generate a new effective antioxidant with therapeutic application for oxidative-stress-related events, namely neurodegenerative diseases.

1. Introduction

Aerobic organisms produce reactive species (RS) during physiological processes, namely by ATP synthesis in the mitochondria, long chain fatty acid degradation in peroxisomes and by enzymatic systems (e.g. NAD(P)H oxidase, xanthine oxidase (XO), nitric oxide synthase).^{1,2} In low/moderate levels, maintained by endogenous antioxidants, RS have an important role in cell signaling and immune response.^{3,4} However, RS overproduction and/or the impairment of antioxidant defenses leads to the oxidative modification biomolecules, a process that significantly contributes for the progression of several pathologies, such as cancer, diabetes, cardiovascular and neurodegenerative diseases (ND).³

The vulnerability of the human brain to oxidative stress is due to a high oxygen consumption, low pool of antioxidant enzymes (e.g. catalase, glutathione peroxidase) and high content in polyunsaturated fatty acids and transition metals (e.g. iron, copper).^{5,6} The data acquired so far strongly supports the hypothesis that oxidative stress plays an important role on neurodegeneration.^{6,7} In fact, neuronal mitochondrial dysfunction leads to RS overproduction, ATP depletion and Ca²⁺ deregulation, compromising the cell function. All together these processes lead to the activation of cell death mechanisms.^{8,9} Microglial activation, in response to protein accumulation, also contributes to RS production in the neuronal microenvironment.¹⁰ In this context, the use of exogenous antioxidants able to reach the target sites within the central nervous system (CNS) can be an effective therapeutic approach to delay or prevent oxidative damage.¹¹

Polyphenols represent a structurally heterogeneous group of dietary antioxidants involved in several biological processes in plants, including growth, lignification, pigmentation, pollination and resistance against pathogens, predators and environmental stress.¹² In the organism, polyphenols have a wide range of biological effects which have been ascribed to their antioxidant activity.¹³ These actions include, among others, antibacterial, anti-

inflammatory, antiviral, antithrombotic and neuroprotective activities.^{13,14} The mechanisms underlying the antioxidant activity of polyphenols comprise free radical scavenging and/or indirect actions, such as chelation of transition metals,¹⁵ modulation of gene expression (e.g. ARE/Nrf2 pathway^{1,16}) and inhibition of RS-overproducing enzymes (e.g. XO^{17,18}).

In spite of the existence of an inverse correlation between the consumption of polyphenol enrich foods and the incidence of oxidative stress-related diseases,^{19,20} the physicochemical properties of polyphenols significantly limit their bioavailability.²¹ In general, phenolic compounds are poorly absorbed and highly metabolized and excreted.²² In this sense, the structural refinement of polyphenols to enhance their absorption, distribution, metabolism and excretion (ADME) is a valid approach to improve their efficacy and therapeutic potential.²³

Polyphenols can be classified based on chemical structure and can be divided in two main groups: flavonoids and non-flavonoids.²⁴ Phenolic acids are non-flavonoid compounds containing one or more phenolic functions and a carboxylic acid group.²⁵ This subclass is classically subdivided in hydroxybenzoic (Figure 1a) and hydroxycinnamic acids (HCAs) (Figure 1b).^{21,26} Cinnamic acid is a versatile scaffold that has been exploited in several drug discovery and development programs. Several structural modifications have been performed to raise its lipophilicity (e.g. by esterification^{27,28}, by amidation⁷ and by coupling with lipophilic cations²⁹), while preserving or improving the biological activity, for instance the antioxidant properties.²³

As part of our project related with the development of potent and effective antioxidants based on natural models, we report the first studies implemented to evaluate the influence of the extension of the ethylenic spacer between the aromatic ring and the carboxylic acid of the cinnamic scaffold (Figure 1c) in the antioxidant profile by the assessment of physicochemical and biological properties using *in vitro* and *in silico* methodologies. The evaluated parameters include the radical scavenging activity (DPPH[•], ABTS^{•+} and GO[•]), redox properties, iron (II) chelating activity,

octanol/water partition coefficient (cLogP), cytotoxicity and neuroprotection in a cellular model. The performance of the synthesized compounds will be compared with that of the naturally occurring cinnamic acids. At the end the study may provide relevant information for the development of new chemical entities for targeting the central nervous system (CNS).

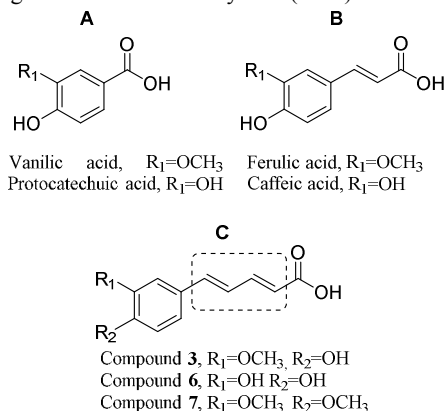


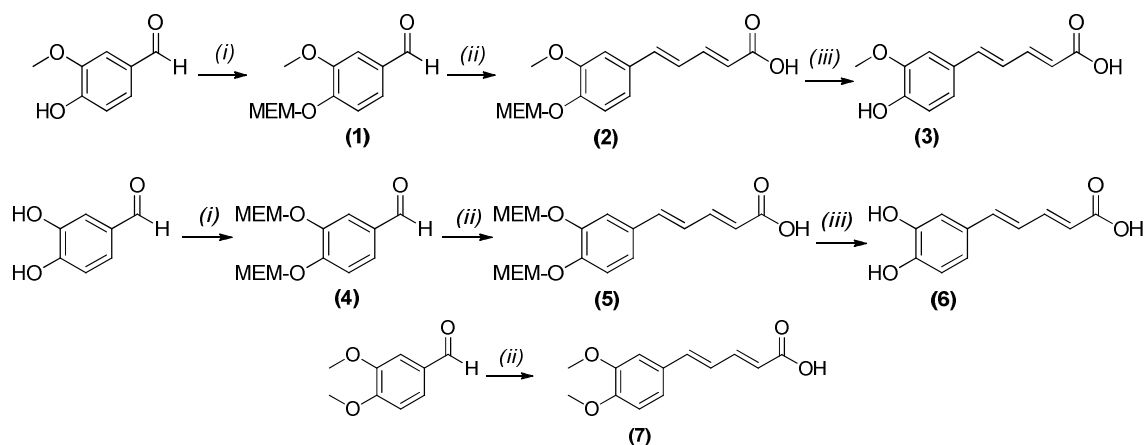
Figure 1. Chemical structure of some hydroxybenzoic (**a**) and hydroxycinnamic acids (**b**) existent in Nature. (**c**) HCA derivatives developed by bioinspired synthesis.

2. Results and discussion

2.1. Chemistry

Phenol protection and deprotection are useful tools on the synthesis of natural products and their derivatives, often used not only to minimize reactivity of the hydroxyl group, but also to improve the selectivity of the subsequent reaction. Following the designated approach compounds **3** and **6** were synthesized in a three-step strategy, as depicted in Scheme 1. Firstly, the alkylation of the hydroxyl function(s) with 2-methoxyethoxymethyl chloride (MEMCl) in the presence of a weak base (diisopropylethylamine,

DIPEA) and a source of iodide (tetrabutylammonium iodide, TBAI), provided the MEM-protected phenols (step *i*, compounds **1** and **4**, Scheme 1). The protection step was found to be crucial, since all attempts to build the extended tether with free OH functions were unsuccessful. The introduction of the spacer was carried out by reaction between the protected compounds **1** and **4** with ethyl crotonate in *N*-methyl-2-pyrrolidinone (NMP) in basic conditions (step *ii*, Scheme 1). The final compounds (**3** and **6**, Scheme 1) were obtained after the removal of MEM group using Amberlyst® 15 cation exchanger in methanol/water (95:5) (step *iii*, Scheme 1). The synthesis of compound **7** involved only the spacer introduction (step *ii*), as the phenolic functions were already protected. Phenol protection (step *i*, compounds **1** and **4**) occurred in mild conditions with high yields (85 to 90 %), and MEM-protected phenols were easily purified. However, the products resulting from the spacer introduction with MEM-protected phenols (step *ii*, compounds **2** and **5**) were obtained with lower yields (56 to 58 %) compared to compound **7** (72 %). In fact, the reactions of the MEM-protected compounds with ethyl crotonate were not complete, suggesting that this group might affect the reactivity of the aldehyde function. Finally, the removal of the protecting group from compounds **2** and **5** (step *iii*) and obtention of compounds **3** and **6** occurred with low yields (10 to 23 %). The increased electron delocalization derived from spacer introduction might decrease the acid-labile properties of MEM. Recently, Li *et al.* reported the synthesis of compound **3**³⁰ in a strategy that includes acetylation, chain elongation and hydrolysis processes. Yet, the procedure encloses a previous preparation of the elongating reagent. The synthetic strategy herein described involved milder conditions and a reduced number of steps being cheaper, as less reagents and purifications procedures were required, and environmentally friendly, particularly due to the use of a water-compatible recyclable resin in the deprotection step. Structural characterization of the synthesized compounds and their intermediates was performed by NMR spectroscopy (¹H and ¹³C NMR and DEPT). The final compounds were also characterized by mass spectrometry (EI-MS).



Scheme 1: Synthesis of cinnamic acid derivatives. (*i*) MEMCl, DIPEA, TBAI; CH_2Cl_2 , (*ii*) ethyl crotonate, NMP, *t*-BuOK; (*iii*) Amberlyst® 15, MeOH/H₂O (95:5).

2.2. Evaluation of radical scavenging activity

Polyphenols exert their radical scavenging activity by transferring a hydrogen atom or an electron to an unstable free radical.³¹ In this process, the resulting phenoxyl radical is less likely to propagate

further radical reactions due to the electron delocalization throughout the aromatic ring.³¹ The radical scavenging activity of hydroxycinnamic acid derivatives was accessed by DPPH[•], ABTS^{•+} and GO[•] assays. All these methods involved the spectrophotometric measurement of the absorbance decrease resulting from radical deactivation by an antioxidant. The results were expressed as IC₅₀, which is defined as the minimum antioxidant concentration necessary to reduce the amount of radical by 50 %. Ferulic acid (FA), caffeic acid (CA) and trolox (TRX) were used as reference scavengers. In addition, the activity of the cinnamic acid precursor (3,4-dimethoxycinnamic acid, DMC) of compound 7 was also evaluated. Compounds with higher antioxidant activity display lower IC₅₀ values.

Table 1. Radical scavenging activities and redox potentials (E_p) of cinnamic acids and their derivatives. Radical scavenging activity results are expressed as mean IC₅₀ ± standard deviation (n=3). n.a.: not active.

Compound	IC ₅₀ /μM			E_p /mV
	DPPH [•]	ABTS ^{•+}	GO [•]	
FA	49.3±1.7	23.9±0.8	26.5±0.81	346; 440
CA	21.7±0.2	17.5±0.2	2.7±0.11	168
DMC	n.a.	n.a.	n.a.	1071
3	43.5±2.5	19.7±0.3	4.8±0.06	299; 516
6	18.2±0.2	11.1±0.7	2.5±0.05	155
7	>75	> 50	n.a.	868; 1040
TRX	30.8±0.1	28.7±0.6	3.4±0.1	-

Overall from the results shown in Table 1, it can be observed that CA and compound 6 display lower IC₅₀ values than FA and compound 3, respectively. On the other hand, compound 7 did not show any significant radical scavenging activity.

Particularly from the DPPH[•] assay (Table 1 and Figure 2a) it was found that the IC₅₀ obtained for compound 3 is significantly lower ($p < 0.01$) than the naturally occurring analogue (FA), indicating an enhancement of antioxidant activity in this *in vitro* model. This trend was also observed for the 6/CA pair, with a significant increase observed for derivative 6 ($p < 0.001$). Moreover, compound 6 was more effective than the reference compound TRX (Figure 2a). Similarly, results from the ABTS^{•+} assay showed that a decrease of the IC₅₀ values (Table 1 and Figure 2b) was observed with the introduction of an additional double bond between the aromatic ring and the carboxylic acid group. The improvement of antioxidant activity was statistically significant for both pairs (compound 3/FA and compound 6/CA, $p < 0.001$, Figure 2b). All the compounds displayed higher ABTS^{•+} scavenging activity than the reference antioxidant TRX (Figure 2b). Finally, the IC₅₀ values for compound 6 and CA were statistically similar in the GO[•] assay (Figure 2c and Table 1). Moreover, the GO[•] scavenging activity of compound bearing a catechol group was significantly higher than the reference antioxidant (TRX vs CA: $p < 0.05$, TRX vs compound 6: $p < 0.01$, Figure 2c). Lastly, a significant improvement on the radical scavenging activity on the FA/3 pair was observed ($p < 0.001$). Overall, these results suggest that the presence of hydroxyl groups attached to the aromatic ring, preferentially a catechol system, is important for the enhancement of the radical scavenging activity of

cinnamic based compounds. In general, the introduction of an extra double bond (C=C) may contribute for the extension of the electronic delocalization, enhancing the stability of the radical intermediate and improving radical scavenging ability. These results are in accordance with previous reports.^{15,32,33}

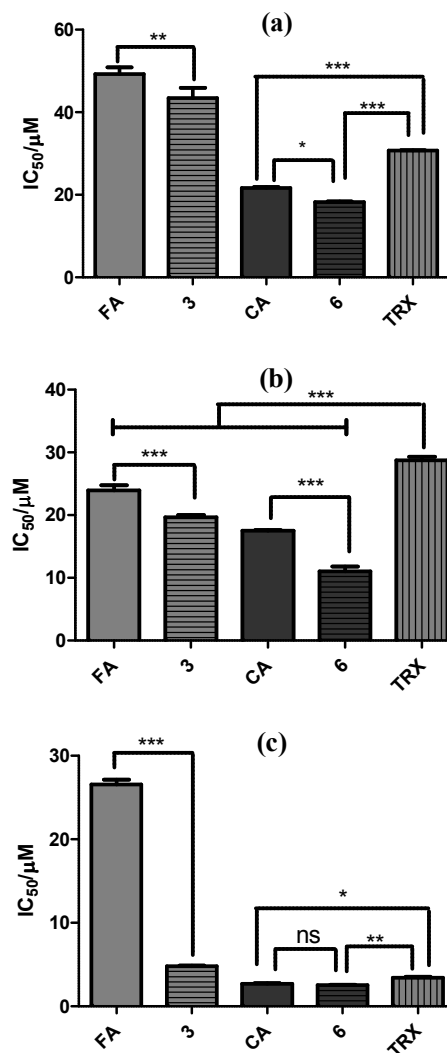


Figure 2. Statistical analysis of IC₅₀ values obtained for cinnamic acids and their derivatives on (a) DPPH[•], (b) ABTS^{•+} and (c) GO[•] assays. Results are expressed as mean IC₅₀ ± standard deviation (n=3). (n.s. non-significant, * $p < 0.05$, ** $p < 0.01$; *** $p < 0.001$)

2.3. Evaluation of iron (II) chelation properties

The ability of transition metals (e.g. iron) to adopt multiple valence states and to participate in redox cycles is recognized by enzymatic systems in the activation or transfer of molecular oxygen. However, their metabolic deregulation and intra- and extracellular accumulation may result in oxidative damage.³⁴ Iron is important for brain oxygen transport, electron transfer and neurotransmitter synthesis. In the brain, iron levels increase with age and it has been observed that free iron or iron overload is a putative factor in the pathogenesis of chronic neurologic disorders including Alzheimer's and Parkinson's disease.³⁵ It has been demonstrated that excessive iron can lead to free radical production, which can promote neurotoxicity.¹ In this context, the use of metal chelating agents, or

antioxidants that operate by more than one mechanism, can function as an alternative therapeutic approach to prevent metal-induced neurotoxicity. Thus, the iron (II) chelating properties of HCA derivatives were evaluated by the ferrozine assay. This method is based on the spectrophotometric monitoring of $[\text{Fe}(\text{ferrozine})_3]^{2+}$ complex formation at 562 nm, which is prevented in presence of a chelator that competes with ferrozine for the iron in solution. Accordingly, a decrease in absorbance is observed when compounds with chelating activity are added to the solution. The percentage of iron (II) chelation for the tested compounds is depicted in Figure 3. EDTA was used as reference.

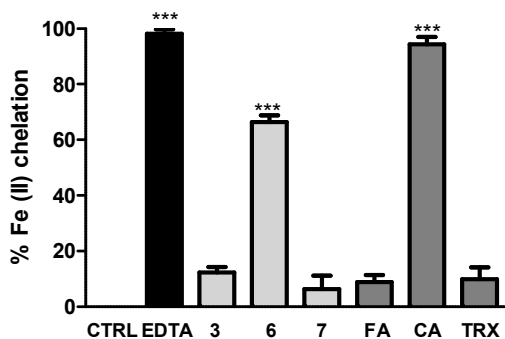


Figure 3. Iron (II) chelation activity cinnamic acids and their derivatives. Results are expressed as mean % Fe (II) chelation \pm standard deviation ($n=3$). (n.s. non-significant, $*p < 0.05$, $**p < 0.01$; $***p < 0.001$)

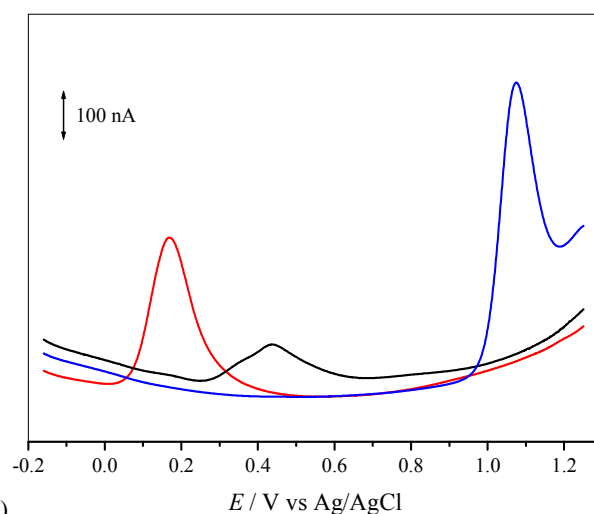
Catecholic compounds (compound 6 and CA) were better iron (II) chelators than monophenolic compounds (compound 3, FA and TRX), which showed only residual chelation properties. In this case, the presence of the additional double bond does not significantly influence iron (II) chelation capacity. It has been already reported that compounds with two or more hydroxyl groups are more likely to have chelating properties.³⁶ In fact, catechols are described as effective metal chelators because at $\text{pH} \leq 7.4$ they usually form complexes with octahedral geometry involving three molecules bonded to one iron center.³⁷ The postulate was reinforced by the data attained for FA and compound 3, which hold only one hydroxyl group.³⁸

2.4. Evaluation of redox potentials

Among a wide range of applications, voltammetric techniques can also be used for the assessment of antioxidant properties. They are employed as a complementary method as they allow the measurement of redox potentials, and in turn provide additional information about a compound's oxidative behaviour.²⁸ It is by now recognized that redox potentials can be correlated with the antioxidant activity: generally, low oxidation potentials (E_p) are associated with a greater facility or strength of a given molecule for the electron donation and, thus, to act as antioxidant. In this context, differential pulse voltammetry (DPV) and cyclic voltammetry (CV) were used to study the behavior of HCAs and their derivatives at physiological pH. Differential pulse voltammograms of FA and compound 3 presented two overlapped anodic peaks at physiological pH (FA: $E_p = +346$ mV, $E'_p = +440$ mV; compound 3: $E_p = +299$ mV, $E'_p = +516$ mV), both resulting from the oxidation of the phenoxyl group present in their structures (Figure 4). Cyclic voltammograms obtained for both compounds also show the appearance of two overlapped peaks (Figure 5). The anodic waves

appear to correspond to an irreversible process. The gathered data corroborates the results found by other studies regarding ferulic acid behaviour during oxidation.^{7, 28} The proposed mechanism involves a one-electron transfer from the phenolic moiety followed by one irreversible dimerization process due to a radical-radical coupling reaction between two phenoxyl radicals. DPV of CA and compound 6 showed only one anodic wave at physiological pH (CA: $E_p = +168$ mV; compound 6: $E_p = +155$ mV) which can be ascribed to the oxidation of the catechol group (Figure 4). Cyclic voltammograms were also recorded and the data obtained for CA and compound 6 are characteristic of an electrochemical reversible reaction showing only one anodic peak and one cathodic peak on the reverse scan (Figure 5). These results are in agreement with the literature data, which concerns the oxidative behavior of caffeic acid.^{7, 28} Electrochemical studies on the caffeic acid oxidation mechanisms have shown that the first oxidation step involves two electrons per molecule, which likely corresponds to the formation of the caffeic acid ortho-quinone.

(a)



(b)

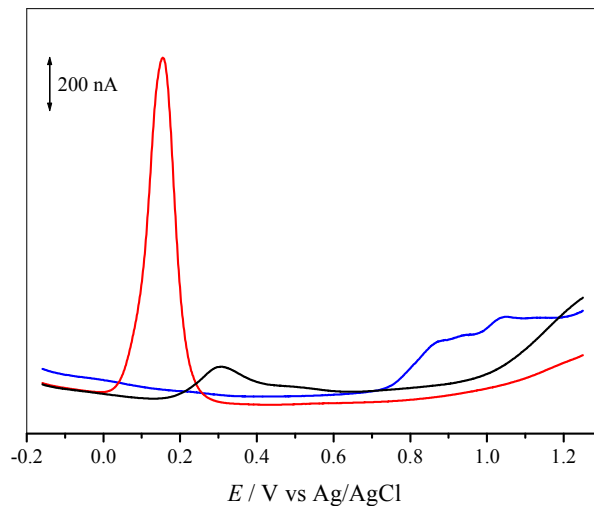


Figure 4. Differential pulse voltammograms of 0.1 mM solutions of (a) (—) FA, (—) CA and (—) DMC; (b) (—) compound 3, (—) compound 6 and (—) compound 7 in pH 7.4 buffer electrolyte. Scan rate: 5 mV s^{-1} .

The differential pulse voltammetric study of DMC and compound 7 revealed the presence of one well-defined anodic peak and two overlapped peaks at physiologic pH, respectively (DMC: $E_p =$

+1071 mV; compound **7**: $E_p = +868$ mV, $E'_p = +1040$ mV) corresponding to the removal of one electron from the aromatic nucleus present in the molecules and subsequent formation of a radical cation (Figure 4). Cyclic voltammograms recorded showed irreversible anodic peaks (Figure 5). These results point out that a very fast subsequent chemical reaction of the radical aromatic cation on the anodic oxidation takes place, so that the reduction of the radical cation will not occur in the time scale of the experiment.^{29, 42} Oxidation potentials of the compounds under analysis are shown in Table 1. Compounds **3**, **6** and **7** exhibit lower E_p values than the corresponding parent cinnamic acids. Furthermore, compounds bearing a catechol group (compound **6** and **CA**) had lower oxidation potentials. Methoxylation of the catechol group of the cinnamic acid shifts the redox potential towards more positive values. The results demonstrated that the electron delocalization and a higher number of hydroxyl groups present in the cinnamic acid scaffold improve antioxidant activity. These observations are in accordance with previous reports.^{7, 28}

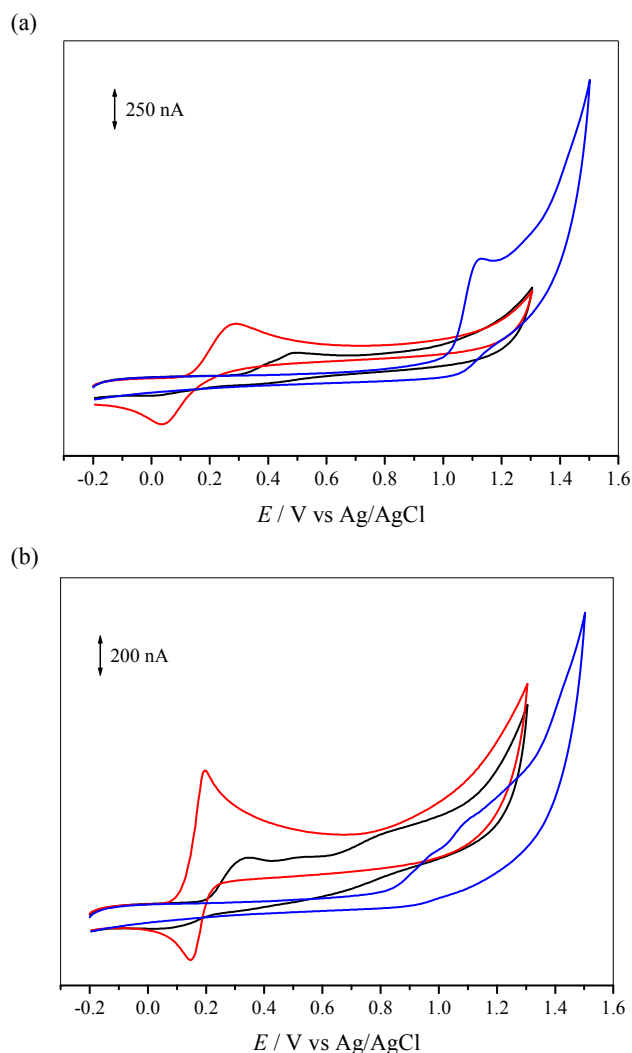


Figure 5. Cyclic voltammograms of 0.1 mM solutions of (a) (—) FA, (—) CA and (—) DMC; (b) (—) compound **3**, (—) compound **6** and (—) compound **7** in pH 7.4 buffer electrolyte. Scan rate: 20 mV s⁻¹.

2.5. Estimation of physicochemical properties

The brain is undoubtedly one of the least accessible organs for the delivery of drugs. The entry and the exit of endogenous and exogenous compounds is controlled by two physiological barriers separating the CNS and the blood supply: blood-brain barrier (BBB) and blood-cerebrospinal fluid barrier (BCSFB). Due to its higher surface area BBB is considered the main region controlling the uptake of drugs into the brain parenchyma and the target for delivering drugs to the brain.³⁹ The transport routes of molecules across the BBB include passive diffusion, transcytosis and carried-protein transport.⁴⁰ Passive diffusion is influenced by the physicochemical properties of the compounds.⁴¹ Generally, CNS targeted drugs show moderate lipophilicity (expressed as the octanol/water partition coefficient, LogP), low molecular weight (MW) and a reduced number of hydrogen bond donors (nOHNH) and acceptors (nON).⁴² Thus, to predict the BBB permeation capacity of the compounds under study the mentioned parameters were calculated (Table 2).

Table 2. Predicted physicochemical properties of cinnamic acids and related derivatives.

Compound	MW	LogP	nON	nOHNH
DMC	208.21	1.56	4	1
FA	194.19	1.25	4	2
CA	180.16	0.94	4	3
7	234.25	2.07	4	1
3	220.22	1.77	4	2
6	206.20	1.46	4	3
CNS ⁺ drugs ⁴²	< 450	< 5	< 7	< 3

From the calculated data it can be concluded that all the compounds are within the range established for brain permeable drugs. The presence of an additional double bond in compounds **3**, **6** and **7** led to an increase of logP and MW, maintaining the number of hydrogen bond donors and acceptors.

Lipophilicity is generally regarded to be one of the most important, if not the most important, physicochemical property in CNS drug discovery and development programs: it is a key determinant of a drug's brain to plasma ratio (K_p) and brain concentration (C_b), which in turn significantly influence its CNS efficacy.⁴³ Since a higher logP value is related to a lower aqueous solubility and high BBB permeability and plasma protein binding,^{44,45} an improvement on the bioavailability of the current HCAs derivatives is expected. Therefore, the elongation of the HCA result in a dual beneficial effect: on one hand, the enhancement of electronic delocalization maintained or improved the antioxidant properties; on the other hand, the increase of compounds' lipophilicity might improve their bioavailability.

2.6. Cytotoxicity and neuroprotection

The cytotoxicity of the HCA derivatives was accessed by the determination of cell viability via MTT reduction assay, which was performed after a 24 h incubation period of the synthesized compounds at two different concentrations with human neuroblastoma cells (SH-SY5Y cell line). The results obtained are shown in Figure 6a. The cell viability was not affected by the presence of test compounds at 1 μ M and 10 μ M when compared to the control. These results suggest that hydroxycinnamic acid derivatives do not exert cytotoxic effects on the studied concentration range. As previous studies advocated that **FA** and **CA**

have neuroprotective properties against oxidative stress^{46–48} the potential neuroprotective activity of the synthesized compounds was evaluated. From the diversity of oxidative stressors 6-hydroxydopamine (6-OH-DA) was used as inducer in the present studies. Due to the structural resemblance with dopamine, 6-OH-DA is transported inside the cells by dopamine transporter and accumulates in the cytosol. This molecule gives rise to free radicals after autooxidation and leads to ATP depletion through inhibition of complexes I and IV of the respiratory chain.^{49,50} Cellular viability was determined after a 24 h incubation period of SH-SY5Y cells with the test compounds, in the presence of 6-OH-DA at 100 μ M. The results obtained are depicted in Figure 6b. As expected, the stress inducer reduced the cell survival to 45.8 ± 7.4 % compared to the control of non treated cells ($p < 0.001$). Compound 6 reduced 6-OH-DA induced cytotoxicity at 1 μ M ($p < 0.001$) and 10 μ M ($p < 0.01$). Compound 3 also reduced cell death, but the cell viability was only statistically different at 10 μ M ($p < 0.05$) compared to incubation with 6-OH-DA. This effect was not observed for compound 7, which did not improve the cell survival of 6-OH-DA treated cells. These results showed a correlation between the number of phenolic functions and the protection against oxidative stress: neuroprotection was observed at high concentrations of monophenolic compound 3, but only the catecholic compound 6 significantly reduced 6-OH-DA induced damage at all tested concentrations and displayed neuroprotective potential under in the current cellular model.

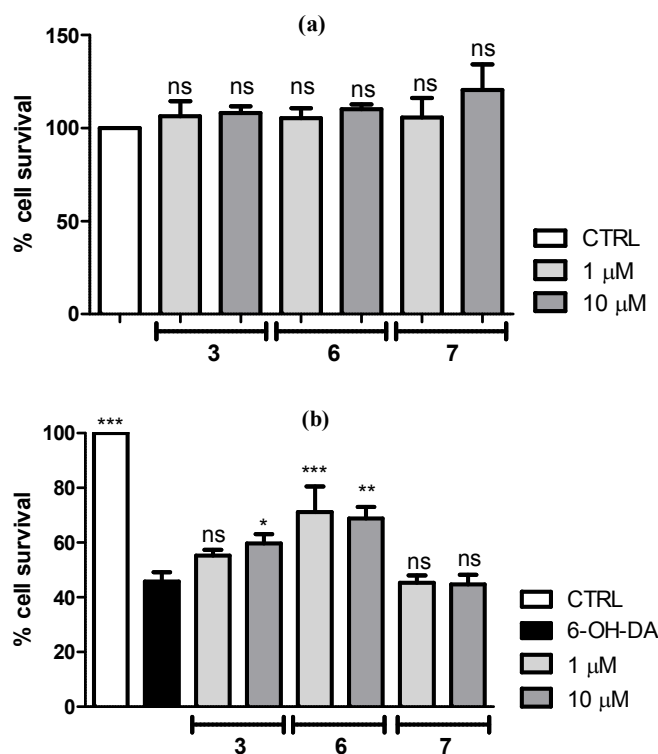


Figure 6. Evaluation of (a) cytotoxic and (b) neuroprotective properties of test compounds in SH-SY5Y cells with two different concentrations. Results are expressed as mean % cell viability \pm standard deviation ($n=3$) (n.s. non-significant, * $p < 0.05$, ** $p < 0.01$, *** $p < 0.001$).

3. Experimental section

3.1. Chemistry. General methods and apparatus

4-Hydroxy-3-methoxybenzaldehyde (vanillin), 3,4-dihydroxybenzaldehyde, 3,4-dimethoxybenzaldehyde, 2-methoxyethoxymethyl chloride (MEMCl), *N,N*-diisopropylethylamide (DIPEA), ethyl crotonate, potassium tert-butoxide (t-BuOK), *N*-methyl-2-pyrrolidinone (NMP), Amberlyst® 15 hydrogen form (dry and wet), ferulic acid (FA), caffeic acid (CA), 3,4-dimethoxycinnamic acid (DMC), (\pm)-6-hydroxy-2,5,7,8-tetramethylchromane-2-carboxylic acid (Trolox, TRX), 2,2-diphenyl-1-(2,4,6-trinitrophenyl)hydrazyl radical (DPPH $^{\bullet}$), 2,2'-azinobis-(3-ethylbenzothiazoline-6-sulfonic acid (ABTS), potassium persulfate, 2,6-di-*tert*-butyl- α -(3,5-di-*tert*-butyl-4-oxo-2,5-cyclohexadien-1-ylidene)-*p*-tolylloxy radical (Galvinoxyl, GO $^{\bullet}$), ammonium acetate, ammonium iron (II) sulfate hexahydrate, (3-(2-pyridyl)-5,6-diphenyl-1,2,4-triazine-4',4''-disulfonic acid sodium salt (Ferrozine) and ethylenediaminetetraacetic acid (EDTA) were purchased from Sigma Aldrich and Alfa-Aesar. All other reagents and solvents were acquired from Panreac and used without additional purification. Deionized water (conductivity < 0.1 mS cm^{-1}) was used throughout all the experiments.

The monitoring of reactions progress was performed by thin layer chromatography (TLC) on precoated silica gel 60 F254 acquired from Merck (Darmstadt, Germany). The TLC spots are visualized under UV detection (254 nm). Organic layers obtained in the extraction step were washed with brine, dried over anhydrous sodium sulphate and concentrated under reduced pressure. Some crude products were purified by column chromatography. Column chromatography was carried out on silica gel 60A acquired from Carlo-Erba Reactifs (SDS, France). The fractions with the desired compound were gathered and concentrated *in vacuo*. The solvents were evaporated using a Buchi Rotavapor.

^1H and ^{13}C NMR data were acquired, at room temperature, on a Bruker AMX 300 spectrometer operating at 400 and 100 MHz, respectively. The chemical shifts are expressed in δ (ppm) values relative to tetramethylsilane (TMS) as internal reference and coupling constants (J) are given in Hz. Electrospray ionization mass spectra (ESI-MS) were carried out on a VG AutoSpec instrument. The data are reported as m/z (% of relative intensity of the most important fragments).

Antioxidant assays were performed in a multiplate reader (Powerwave XS Microplate Reader) of Bio-Tech instruments.

The voltammetric studies were executed using an Autolab PGSTAT 12 potentiostat/galvanostat (Eco-Chemie, Netherlands) and a one compartment glass electrochemical cell. The voltammetric data was acquired at room temperature using a three-electrode system: a glassy carbon working electrode (GCE) ($d = 2$ mm), a platinum wire counter electrode and an Ag/AgCl saturated KCl reference electrode (Metrohm, Switzerland). A Crison pH-meter with glass electrode was used for the pH measurements (Crison, Spain).

In cell-based assays, cells were incubated in a humidified incubator Hera Cell 150i with 5 % CO_2 at 37 $^{\circ}\text{C}$. Absorbance measurements were carried out in a microplate reader SunriseTM.

3.1.1. Synthesis

General procedure for phenol protection. In a cooled round bottom flask with the phenol (1 mmol) and tetrabutyl ammonium iodide (0.05 mmol per OH) dissolved in dichloromethane (15 mL), DIPEA (2 mmol per OH) and MEMCl (1.5 mmol per OH) were slowly added. The mixture was stirred for 3–4 h at 0 $^{\circ}\text{C}$, then quenched with water and extracted with dichloromethane (3×15 mL). The crude product was purified by column chromatography (ethyl acetate/dichloromethane (3:7)) and monitored by TLC (ethyl

acetate/dichloromethane (3:7)). The procedure was adapted from the literature.⁵¹

General procedure for chain elongation. MEM-protected aldehydes or 3,4-dimethoxybenzaldehyde (1 mmol) were dissolved in NMP (1.3 mL). *t*-BuOK (1.2 mmol) and ethyl crotonate (1.34 mmol) were then added and the mixture was stirred at room temperature overnight. The products were purified by column chromatography (ethyl acetate/dichloromethane (3:7)) and recrystallization. The procedure was adapted from the literature⁵². Reaction progress was monitored by TLC (ethyl acetate/dichloromethane (3:7)).

General procedure for MEM deprotection. MEM-protected compounds (1 mmol) were dissolved in MeOH/H₂O (95:5) (20 mL) and Amberlyst® 15 hydrogen form was added. The mixture was stirred at 40 °C protected from light. Upon completion, the mixture was filtered to remove the resin residues and methanol was evaporated under reduced pressure. After addition of HCl 1M at 0 °C, a solid is obtained that was isolated by filtration. The procedure was adapted from the literature⁵³. Reaction progress was monitored by TLC (ethyl acetate/dichloromethane (3:7) or dichloromethane/methanol (9:1)).

3-methoxy-4-((2-methoxyethoxy)methoxy)benzaldehyde (1). Compound **1** was obtained by the general phenol protection protocol in the following conditions: 4-hydroxy-3-methoxybenzaldehyde (0.50 g; 3.3 mmol) dichloromethane (15 mL), DIPEA (1.174 mL; 6.57 mmol), MEMCl (563 µL; 6.57 mmol) and TBAI (0.06 g, 0.16 mmol). Yield (%): 92.4. ¹H NMR (400 MHz, CDCl₃) δ (ppm): 3.36 (s, 3H, O(CH₂)₂OCH₃), 3.56 (m, 2H, OCH₂CH₂OCH₃), 3.88 (m, 2H, OCH₂CH₂OCH₃), 3.94 (s, 3H, OCH₃); 5.42 (s, 2H, OCH₂O), 7.32 (d, *J* = 8.7 Hz, 1H, H(5)), 7.43 (m, 2H, H(2), H(6)), 9.87 (s, 1H, CHO). ¹³C NMR (100 MHz, CDCl₃) δ (ppm): 55.93 (OCH₃), 58.88 (O(CH₂)₂OCH₃), 68.17 (OCH₂CH₂OCH₃), 71.38 (OCH₂CH₂OCH₃), 93.93 (OCH₂O), 109.53 (C(2)), 114.82 (C(5)), 126.30 (C(6)), 131.07 (C(1)), 150.03 (C(3)), 151.92 (C(4)), 190.89 (CHO).

(2E,4E)-5-(3-methoxy-4-((2-methoxyethoxy)methoxy)phenyl)-penta-2,4-dienoic acid or 3-methoxy-4-((2-methoxyethoxy)methoxy)cinnamylideneacetic acid (2). Compound **2** was obtained by the general procedure for chain elongation in the following conditions: compound **1** (0.73 g; 3.0 mmol), NMP (4 mL), *t*-BuOK (0.43 g; 3.8 mmol) and ethyl crotonate (514 µL, 4.1 mmol). Upon completion, dichloromethane (30 mL) was added and the mixture was extracted with NaHCO₃ solution (4×10 mL). The combined aqueous layers were acidified with HCl 1M and extracted with dichloromethane (4×10 mL). The final organic layer was then washed with water (10 mL) and brine (3×10 mL). The final compound was purified by column chromatography. Compound **2** was recrystallized from dichloromethane/*n*-hexane. Yield (%): 56.1. ¹H NMR (400 MHz, CDCl₃) δ (ppm): 3.37 (s, 3H, O(CH₂)₂OCH₃), 3.56 (m, 2H, OCH₂CH₂OCH₃), 3.87 (m, 2H, OCH₂CH₂OCH₃), 3.92 (s, 3H, OCH₃); 5.34 (s, 2H, OCH₂O), 5.71 (d, *J* = 11.1 Hz, 1H, Hδ), 6.84 (m, 2H, Hα, Hγ), 7.06 (m, 2H, H(2), H(6)), 7.19 (d, *J* = 8.9 Hz, 1H, H(5)), 7.97 (ddd, *J* = 1.0 Hz, 11.3 Hz, 14.6 Hz, 1H, Hβ). ¹³C NMR (100 MHz, CDCl₃) δ (ppm): 56.02 (OCH₃), 59.03 (O(CH₂)₂OCH₃), 67.96 (OCH₂CH₂OCH₃), 71.54 (OCH₂CH₂OCH₃), 94.29 (OCH₂O), 110.15 (C(2)), 115.35 (C(5)), 116.09 (Cδ), 121.64 (C(6)), 123.49 (Cβ), 130.71 (C(1)), 142.40

(Cα), 147.33 (Cγ), 147.83 (C(3)), 149.82 (C(4)), 170.72 (COOH).

(2E,4E)-5-(4-hydroxy-3-methoxyphenyl)penta-2,4-dienoic acid or 4-hydroxy-3-methoxycinnamylideneacetic acid (3). Compound **3** was obtained by the general MEM deprotection protocol in the following conditions: compound **2** (0.53 g; 1.7 mmol), MeOH/H₂O (95:5) (35 mL) and Amberlyst® 15 hydrogen form, dry (1.7 g). The mixture was stirred at 40 °C for 7 h and at room temperature overnight, protected from light. Yield (%): 23.5. ¹H NMR (400 MHz, DMSO-*d*₆) δ (ppm): 3.80 (s, 3H, OCH₃); 5.60 (d, *J* = 11.2 Hz, 1H, Hδ), 6.78 (t, *J* = 11.5 Hz, 1H, Hγ), 6.87 (d, *J* = 15.7 Hz, 1H, Hα), 6.82 (d, *J* = 8.1 Hz, 1H, H(5)), 6.99 (dd, *J* = 1.7 Hz, 8.1 Hz, 1H, H(6)), 7.04 (d, *J* = 1.7 Hz, 1H, H(2)), 7.97 (dd, *J* = 11.7 Hz, 15.7 Hz, 1H, Hβ), 9.43 (s, 1H, OH), 12.16 (s, 1H, COOH). ¹³C NMR (100 MHz, DMSO-*d*₆) δ (ppm): 56.05 (OCH₃), 111.36 (C(2)), 116.34 (C(5)), 117.11 (Cδ), 121.39 (C(6)), 122.32 (Cβ), 128.11 (C(1)), 141.84 (Cα), 145.28 (Cγ), 148.31 (C(3)), 148.59 (C(4)), 167.95 (COOH). EI/MS *m/z* (%): 219.9 (M⁺, 100), 202.9 (8), 186.9 (5), 174.9 (97), 159.9 (57), 142.9 (51), 130.9 (49), 115.0 (96), 109.9 (9), 103.0 (33), 89 (14), 77.0 (37), 65.1 (14), 55.0 (12.4). mp (°C): [184-185].

3,4-bis((2-methoxyethoxy)methoxy)benzaldehyde (4). Compound **4** was obtained by the general phenol protection protocol in the following conditions: 3,4-dihydroxybenzaldehyde (1.00 g; 7.3 mmol) dichloromethane (25 mL), DIPEA (5.170 mL; 29.08 mmol), MEMCl (2.480 mL; 21.81 mmol) and TBAI (0.27 g; 0.73 mmol). Yield (%): 84.0. ¹H NMR (400 MHz, CDCl₃) δ (ppm): 3.37 (s, 3H, O(CH₂)₂OCH₃), 3.38 (s, 3H, O(CH₂)₂OCH₃), 3.56 (m, 4H, 2×OCH₂CH₂OCH₃), 3.87 (m, 4H, OCH₂CH₂OCH₃), 5.37 (s, 2H, OCH₂O), 5.41 (s, 2H, OCH₂O), 7.33 (d, *J* = 8.4 Hz, 1H, H(5)), 7.52 (dd, *J* = 1.9 Hz, 8.4 Hz, 1H, H(6)), 7.71 (d, *J* = 1.9 Hz, 1H, H(2)), 9.87 (s, 1H, CHO). ¹³C NMR (100 MHz, CDCl₃) δ (ppm): 59.95 (OCH₃), 59.98 (OCH₃), 69.08 (OCH₂CH₂OCH₃), 69.15 (OCH₂CH₂OCH₃), 72.35 (OCH₂CH₂OCH₃), 72.40 (OCH₂CH₂OCH₃), 94.87 (OCH₂O), 95.36 (OCH₂O), 116.38 (C(2)), 117.34 (C(5)), 127.10 (C(6)), 132.08 (C(1)), 143.29 (C(3)), 153.53 (C(4)), 192.74 (CHO).

(2E,4E)-5-(3,4-bis((2-methoxyethoxy)methoxy)phenyl)penta-2,4-dienoic acid or 3,4-bis(methoxy-4-((2-methoxyethoxy)methoxy)cinnamylideneacetic acid (5). Compound **5** was obtained by the general procedure for chain elongation in the following conditions: compound **4** (1.67 g; 5.3 mmol), NMP (7 mL), *t*-BuOK (0.72 g; 6.38 mmol) and ethyl crotonate (896 µL, 7.1 mmol). Upon completion, dichloromethane (45 mL) was added and the mixture was extracted with NaHCO₃ solution (3×20 mL). The combined aqueous layers were acidified with HCl 1M and extracted with ethyl acetate (3×20 mL). The final organic layer was then washed with water (10 mL) and brine (3×10 mL). The purification was performed by column chromatography. Compound **5** was recrystallized from dichloromethane/petroleum ether. Yield (%): 58.1. ¹H NMR (400 MHz, CDCl₃) δ (ppm): 3.40 (s, 3H, O(CH₂)₂OCH₃), 3.41 (s, 3H, O(CH₂)₂OCH₃), 3.58 (m, 4H, 2×OCH₂CH₂OCH₃), 3.87 (m, 4H, 2×OCH₂CH₂OCH₃), 5.32 (s, 2H, OCH₂O), 5.33 (s, 2H, OCH₂O), 5.72 (d, *J* = 11.3 Hz, 1H, Hδ), 6.74 (m, 2H, Hα, Hγ), 7.18 (m, 2H, H(5), H(6)), 7.31 (d, *J* = 1.2 Hz, 1H, H(2)), 8.00 (ddd, *J* = 1.0 Hz, 11.4 Hz, 14.6 Hz, 1H, Hβ). ¹³C NMR (100 MHz, CDCl₃) δ (ppm): 59.04 (O(CH₂)₂OCH₃), 59.05 (O(CH₂)₂OCH₃), 67.97 (OCH₂CH₂OCH₃), 68.00 (OCH₂CH₂OCH₃), 71.55 (2×OCH₂CH₂OCH₃), 94.26 (OCH₂O), 94.74 (OCH₂O) 115.74

(C(2)), 116.56 (C(5)), 116.59 (C(8)), 122.28 (C(6)), 123.88 (C(β)), 130.93 (C(1)), 142.04 (C(α)), 147.15 (C(γ)), 147.29 (C(3)), 148.45 (C(4)), 170.93 (COOH).

(2E,4E)-5-(3,4-di-hydroxyphenyl)penta-2,4-dienoic acid or 3,4-di-hydroxycinnamylideneacetic acid (6). Compound 6 was obtained by the general MEM-deprotection protocol in the following conditions: compound 5 (0.79 g; 2.1 mmol), MeOH/H₂O (95:5) (35 mL) and Amberlyst® 15 hydrogen form, wet (2.1 g). The mixture was stirred for 48 hours protected from light, at 40 °C for 20 h and at room temperature overnight. Additional aliquots of Amberlyst® 15 hydrogen form, wet (4.2 g, 4.0 g and 4.6 g) were added until product formation was detected by TLC. Yield (%): 10.7. ¹H NMR (400 MHz, DMSO-*d*₆) δ (ppm): 5.58 (d, *J* = 11.1 Hz, 1H, Hδ), 6.77 (m, 4H, H(5), Hγ, H(6), Hα), 6.98 (d, *J* = 1.9 Hz, 1H, H(2)), 7.79 (ddd, *J* = 0.8 Hz, 11.5 Hz, 15.6 Hz, 1H, Hβ), 9.37 (s, 2H, 2×OH). ¹³C NMR (100 MHz, DMSO-*d*₆) δ (ppm): 113.66 (C(2)), 116.35 (C(5)), 116.97 (C(8)), 120.77 (C(6)), 122.04 (C(β)), 128.14 (C(1)), 141.78 (C(α)), 145.25 (C(γ)), 146.11 (C(3)), 147.64 (C(4)), 168.12 (COOH). *EI/MS* *m/z* (%): 205.9 (M⁺, 68), 160.9 (100), 142.9 (23), 132.0 (910), 115.0 (53), 103 (9), 89.0 (9), 77 (8), 59 (4). mp (°C): [174-175]

(2E,4E)-5-(3,4-dimethoxyphenyl)penta-2,4-dienoic acid or 3,4-dimethoxycinnamylideneacetic acid (7). Compound 7 was obtained by the general procedure for chain elongation in the following conditions: 3,4-dimethoxybenzaldehyde (1.01 g; 6.1 mmol), NMP (5 mL), *t*-BuOK (0.80 g; 7.1 mmol) and ethyl crotonate (1 mL, 8.0 mmol). Upon completion, the mixture was neutralized with HCl 1M and extracted with dichloromethane (3×15 mL). The organic layer was extracted with NaOH 2M and the resulting aqueous layer was neutralized with HCl 1M. The solid product was isolated by filtration. Yield (%): 72.9. ¹H NMR (400 MHz, DMSO-*d*₆) δ (ppm): 3.79 (s, 3H, OCH₃), 3.80 (s, 3H, OCH₃), 5.65 (d, *J* = 11.2 Hz, 1H, Hδ), 6.80 (t, *J* = 11.32, 1H, Hγ), 6.91 (d, *J* = 15.7 Hz, 1H, Hα), 6.98 (d, *J* = 8.2 Hz, 1H, H(5)), 7.09 (m, 2H, H(2), H(6)), 7.88 (dd, *J* = 11.5 Hz, 15.7 Hz, 1H, Hβ), 12.22 (s, 1H, COOH). ¹³C NMR (100 MHz, DMSO-*d*₆) δ (ppm): δ (ppm) = 55.93 (OCH₃), 56.02 (OCH₃), 110.5 (C(2)), 112.41 (C(5)), 117.69 (C(8)), 121.16 (C(6)), 123.14 (C(β)), 129.40 (C(1)), 141.39 (C(α)), 145.02 (C(8)), 149.40 (C(3)), 150.39 (C(4)), 167.89 (COOH). *EI/MS* *m/z* (%): 233.9 (M⁺, 81), 189.0 (100), 173.9 (30), 158.0 (29), 145.0 (11), 127.0 (9), 115.0 (31), 103.0 (18), 91.0 (8), 77.0 (14), 63.0 (5). mp (°C): [137-141].

3.2. Radical scavenging activity

The radical scavenging activity of the synthesized compounds was evaluated by DPPH[•], ABTS^{•+} and GO[•] assays. The results were expressed in IC₅₀ as mean ± standard deviation (*n* = 3). TRX, a water-soluble vitamin E derivative, was used as a standard reference.

DPPH[•] radical assay. DPPH[•] radical scavenging activity was performed as previously described²⁷. Briefly, solutions of the test compounds with increasing concentrations (range between 10 μM and 750 μM) were prepared in ethanol. A DPPH[•] ethanolic solution (6.85 μM) was also prepared and then diluted to reach the absorbance of 0.72 ± 0.02 at 515 nm. Each compound solution (20 μL) was added to 180 μL of DPPH[•] solution in triplicate, and the absorbance at 515 nm was recorded minutely

over 45 minutes. The percent inhibition of radical was based on comparison between the blank (20 μL of ethanol and 180 μL of DPPH[•] solution), which corresponds to 100 % of radical, and test compounds solutions. The dose-response curves allowed the determination of IC₅₀ values.

ABTS^{•+} radical cation assay. ABTS^{•+} scavenging activity was evaluated as previously described²⁷. Briefly, ethanolic solutions of the test compounds with increasing concentrations (range between 50 μM and 500 μM) were prepared. ABTS^{•+} radical cation solution was obtained by addition of 150 mM aqueous potassium persulfate solution (163 μL) to 10 mL of 7 mM aqueous ABTS solution followed by storage in the dark at room temperature for 16 h (2.45 mM final concentration). The solution was then diluted in ethanol to reach the absorbance of 0.72±0.02. After addition, in triplicate, of compound solution (20 μL) to ABTS^{•+} solution (180 μL) the spectrophotometric measurement was carried out minutely over 15 minutes. The percent inhibition of radical was based on comparison between the blank (20 μL of ethanol and 180 μL of ABTS^{•+} solution), which corresponds to 100 % of radical, and test compounds solutions. The dose-response curves allowed the determination of IC₅₀ values.

GO[•] radical assay. GO[•] radical scavenging protocol was adapted from the literature⁵⁴⁻⁵⁶. Solutions of test compounds with concentrations from 5 μM to 350 μM were prepared in ethanol. An ethanolic solution of 5 mM GO[•] was prepared and diluted to reach the absorbance of 1.00 ± 0.02 at 428 nm. The addition (20 μL) in triplicate of compound solution to GO[•] solution (180 μL) was followed by absorbance measurement at 428 nm over 30 minutes, in the dark, at room temperature. The percent inhibition of radical was based on comparison between the blank (20 μL of ethanol and 180 μL of GO[•] solution), which corresponds to 100 % of radical, and test compounds solutions. The dose-response curves allowed the determination of IC₅₀ values.

3.3. Electrochemical measurements

Differential pulse voltammetry (DPV) and cyclic voltammetry (CV) procedures were performed as described elsewhere.²⁸ In the electrochemical cell, ethanolic solutions of test compounds 10 mM (100 μL) were diluted in a supporting electrolyte (10 mL) in order to obtain a final concentration of 100 μM. Scan rates used in DPV and CV electrochemical measurements were, respectively, 5 mV/s and 20 mV/s.

The supporting electrolyte was prepared by dilution of 6.2 mL of dipotassium hydrogen phosphate 0.2 M and 43.8 mL of potassium di-hydrogen phosphate 0.2 M in 100 mL of water.

3.4. Iron (II) chelating capacity

Evaluation of iron (II) chelating properties of compounds was accessed using the ferrozine method as described in the literature.⁵⁷ The first step included the preparation of the following solutions: ammonium iron (II) sulfate hexahydrate 20 μM in ammonium acetate buffer 0.2 M pH 6.7, aqueous solution of ferrozine 5 mM and solutions of test compounds in DMSO. To prevent possible interferences, all the solutions were prepared in plastic material, to circumvent iron contamination. A previous incubation at 37 °C for 10 minutes and measurement of absorbance at 562 nm of the test compounds solution (4 μL) added to ammonium iron (II) sulfate hexahydrate in ammonium acetate buffer (200 μL) was carried out in order to evaluate any signal derived from interactions between

compounds and iron (II). Addition of ferrozine solution (4 μ L) was followed by new incubation at 37 °C for 10 minutes and measurement of $[\text{Fe}(\text{ferrozine})_3]^{2+}$ complex absorbance at 562 nm. In the control test compound solution was replaced by DMSO. EDTA was used as a reference. Percentage of iron chelation (% Fe chelation) values were expressed as mean \pm standard deviation ($n = 3$).

3.5. Estimation of physicochemical properties

Calculation of LogP, simulating partition in an n -octanol/water (1:1, v/v) system, as well as MW, nOHNH and nON was performed using the Molinspiration Cheminformatics® [<http://www.molinspiration.com>].

3.6. Cytotoxicity and neuroprotection.

Cell culture and treatments. The human neuroblastoma was acquired from The American Type Culture Collection (ATCC, Manassas, VA). Cells were maintained in Dulbecco's Modified Eagle's Medium (DMEM/F12) supplemented with Fetal Bovine Serum (FBS, 10 %), Glutamax® (1 %) and penicillin-streptomycin (1 %) (reagents from Gibco). The cells were cultured into 75 cm^2 . The growing medium was changed every 2-3 days and the cultures were subcultured 1:20 once a week.

For experimental purposes, cells were seeded in 24-well plates (10^5 cells/plate), being allowed to attach for 24 h before the incubation with test compounds.

Cell viability assay. In cytotoxicity studies, cells were treated with different concentrations of the test compounds (1 μ M and 10 μ M) in FBS-free medium and incubated for 24 h. In the evaluation of neuroprotective properties, the cells pre-treatment with the test compounds (1 μ M and 10 μ M) for 1 h was followed by a 24 h period of incubation with 6-OH-DA (100 μ M, Sigma) in FBS-free medium. Cell viability was estimated using the MTT assay, a method based on the reduction of the yellow MTT by dehydrogenases from active cells.⁵⁸ The resulting formazan is water insoluble and impermeable to the cell membranes, accumulating in healthy cells.⁵⁹ After the 24 h incubation period with test compounds or test compounds+6-OH-DA, cells were treated with MTT solution (0.5 g/mL in PBS) and incubated for 2.5 h. The MTT solution was removed and the formed formazan crystals were dissolved in DMSO. The absorbance was measured in a microplate reader (measuring filter: 540 nm; reference filter: 690 nm). The measured absorbance is correlated to the amount of produced formazan and thus to the number of living cells.⁶⁰ The percentage of cell viability in the presence of the test compounds was determined relatively to the control experiments. The results are expressed as mean of the % cell survival \pm standard deviation.

3.7. Statistical analysis

The results presented in the previous sections are expressed as mean \pm standard deviation of at least three different experiments (number of experiments n indicated for each case). Statistical comparisons between control and test groups were carried by one-way analysis of variance (ANOVA-1) followed by Dunnett comparison post-test ($\alpha = 0.05$, 95 % confidence intervals). Further details of each specific analysis are expressed in the figures. Differences were considered to be significant for p values lower than 0.05. Plots and statistical analysis were performed using GraphPad Prism 5 ® (GraphPad Software, Inc. La Jolla, CA 92037 USA).

4. Conclusion

HCA derivatives with an enlarged conjugated system were successfully synthesised. The chemical modification introduced in the cinnamic acid scaffold lead to compounds' with an amplified lipophilicity, while the antioxidant activity was increased when compared to natural models (caffeic and ferulic acids). The compounds did not displayed cytotoxicity and a significant neuroprotective effect against 6-OH-DA induced damage was observed. Compound **6** stands out as an efficient radical scavenger and iron (II) chelator that ensures drug-like properties. Moreover, neuroprotection against oxidative damage in a cellular model of PD was observed even at low concentrations (1 μ M), while monophenolic compound **3** only protected the cells from oxidative damage at higher concentrations (10 μ M). Therefore, compound **6** developed by biology-oriented approach combines important features for the development of new effective antioxidants with therapeutic application to neurodegenerative diseases. This promising compound will undergo an optimization process from which a new chemical entity based on the HCA scaffold can emerge, envisaging the development of CNS active drugs.

5. Acknowledgements

The authors thank the Foundation for Science and Technology (FCT) of Portugal (PEst-C/UI0081/2015) and QREN (FCUP-CIQ-UP-NORTE-07-0124-FEDER- 000065) projects and grant of T. Silva (SFRH/BD/79671/2011).

Notes and references

‡These authors contributed equally to this work

^a CIQ/Department of Chemistry and Biochemistry, Faculty of Sciences, University of Porto, 4169-007 Porto, Portugal.

^b Addiction Biology Group, Institute for Molecular and Cell Biology, University of Porto, Rua do Campo Alegre s/n, 4150-180, Porto, Portugal.

^c Department of Chemical Engineering, School of Engineering (ISEP), Polytechnic of Porto, 4200-072 Porto, Portugal.

†Corresponding author: fborges@fc.up.pt

1. H. E. de Vries, M. Witte, D. Hondius, A. J. M. Rozemuller, B. Drukarch, J. Hoozemans and J. Van Horssen, *Free Radic. Biol. Med.*, 2008, **45**, 1375–1383.
2. O. Firuzi, R. Miri, M. Tavakkoli and L. Saso, *Curr. Med. Chem.*, 2011, **18**, 3871–3888.
3. K. Dasuri, L. Zhang and J. N. Keller, *Free Radic. Biol. Med.*, 2013, **62**, 170–185.
4. M. Valko, D. Leibfritz, J. Moncol, M. T. D. Cronin, M. Mazur and J. Telser, *Int. J. Biochem. Cell Biol.*, 2007, **39**, 44–84.
5. K. J. Barnham, C. L. Masters and A. I. Bush, *Nat. Rev.*, 2004, **3**, 205–214.
6. L. Migliore and F. Coppedè, *Mutat. Res.*, 2009, **674**, 73–84.
7. F. M. F. Roleira, C. Siquet, E. Orrù, E. M. Garrido, J. Garrido, N. Milhazes, G. Podda, F. Paiva-Martins, S. Reis, R. Carvalho, E. J. T. da Silva and F. Borges, *Bioorg. Med. Chem.*, 2010, **18**, 5816–5825.
8. R. A. J. Smith, R. C. Hartley, H. M. Cocheme and M. P. Murphy, *Trends Pharmacol. Sci.*, 2012, **33**, 341–352.
9. X. Wang, W. Wang, L. Li, G. Perry, H. Lee and X. Zhu, *Biochim. Biophys. Acta*, 2014, **1842**, 1240–1247.
10. O. Hwang, *Exp. Neurobiol.*, 2013, **22**, 11–17.

11. B. Halliwell, *Biochem. Soc. Trans.*, 2007, **35**, 1147–1150.
12. C. G. Fraga, M. Galleano, S. V. Verstraeten and P. I. Oteiza, *Mol. Aspects Med.*, 2010, **31**, 435–445.
13. M. A. Soobrattee, V. S. Neergheen, A. Luximon-Ramma, O. I. Aruoma and T. Bahorun, *Mutat. Res.*, 2005, **579**, 200–213.
14. A. Ebrahimi and H. Schluesener, *Ageing Res. Rev.*, 2012, **11**, 329–345.
15. M. Leopoldini, N. Russo and M. Toscano, *Food Chem.*, 2011, **125**, 288–306.
16. S. Magesh, Y. Chen and L. Hua, *Med. Res. Rev.*, 2013, **32**, 687–726.
17. Y.-C. Chang, F.-W. Lee, C.-S. Chen, S.-T. Huang, S.-H. Tsai, S.-H. Huang and C.-M. Lin, *Free Radic. Biol. Med.*, 2007, **43**, 1541–1551.
18. H.-C. Lin, S.-H. Tsai, C.-S. Chen, Y.-C. Chang, C.-M. Lee, Z.-Y. Lai and C.-M. Lin, *Biochem. Pharmacol.*, 2008, **75**, 1416–1425.
19. M. Nardini, E. Cirillo, F. Natella and C. Scaccini, *J. Agric. Food Chem.*, 2002, **50**, 5735–5741.
20. J. Bouayed and T. Bohn, *Oxid. Med. Cell. Longev.*, 2010, **3**, 228–237.
21. H. R. El-Seedi, A. M. A. El-Said, S. A. M. Khalifa, U. Göransson, L. Bohlin, A.-K. Borg-Karlson and R. Verpoorte, *J. Agric. Food Chem.*, 2012, **60**, 10877–10895.
22. M. A. Singh, M. Arseneault, T. Sanderson, V. Murthy and C. Ramassamy, *J. Agric. Food Chem.*, 2008, **56**, 4855–4873.
23. S. Benfeito, C. Oliveira, P. Soares, C. Fernandes, T. Silva, J. Teixeira and F. Borges, *Mitochondrion*, 2013, **13**, 427–435.
24. S. Khadem and R. J. Marles, *Molecules*, 2010, **15**, 7985–8005.
25. R. J. Robbins, *J. Agric. Food Chem.*, 2003, **51**, 2866–2887.
26. I. Ignat, I. Volf and V. I. Popa, *Food Chem.*, 2011, **126**, 1821–1835.
27. J. Teixeira, T. Silva, S. Benfeito, A. Gaspar, E. M. Garrido, J. Garrido and F. Borges, *Eur. J. Med. Chem.*, 2013, **62**, 289–296.
28. J. Garrido, A. Gaspar, E. M. Garrido, R. Miri, M. Tavakkoli, S. Pourali, L. Saso, F. Borges and O. Firuzi, *Biochimie*, 2012, **94**, 961–967.
29. J. Teixeira, P. Soares, S. Benfeito, A. Gaspar, J. Garrido, M. P. Murphy and F. Borges, *Free Radic. Res.*, 2012, **46**, 600–611.
30. Y. Li, F. Dai, X. Jin, M. Ma, Y. Wang, X. Ren and B. Zhou, *Food Chem.*, 2014, **158**, 41–47.
31. B. D. Craft, A. L. Kerrihard, R. Amarowicz and R. B. Pegg, *Compr. Rev. Food Sci. Food Saf.*, 2012, **11**, 148–173.
32. A. Gaspar, M. Martins, P. Silva, E. M. Garrido, J. Garrido, O. Firuzi, R. Miri, L. Saso and F. Borges, *J. Agric. Food Chem.*, 2010, **58**, 11273–11280.
33. J. C. J. M. D. S. Menezes, S. P. Kamat, J. A. S. Cavaleiro, A. Gaspar, J. Garrido and F. Borges, *Eur. J. Med. Chem.*, 2011, **46**, 773–777.
34. D. G. Smith, R. Cappai and K. J. Barnham, *Biochim. Biophys. Acta*, 2007, **1768**, 1976–90.
35. F. Carmona, Ó. Palacios, N. Gálvez, R. Cuesta, S. Atrian, M. Capdevila and J. M. Domínguez-Vera, *Coord. Chem. Rev.*, 2013, **257**, 2752–2764.
36. I. Gülçin, *Toxicology*, 2006, **217**, 213–220.
37. N. R. Perron and J. L. Brumaghim, *Cell Biochem. Biophys.*, 2009, **53**, 75–100.
38. S. Maqsood and S. Benjakul, *Food Chem.*, 2010, **119**, 123–132.
39. J. M. Scherrmann, *Vascul. Pharmacol.*, 2002, **38**, 349–354.
40. Y. Chen and L. Liu, *Adv. Drug Deliv. Rev.*, 2012, **64**, 640–665.
41. C. A. Lipinski, F. Lombardo, B. W. Dominy and P. J. Feeney, *Adv. Drug Deliv. Rev.*, 2001, **46**, 3–26.
42. H. Pajouhesh and G. R. Lenz, *NeuroRx*, 2005, **2**, 541–553.
43. Z. Rankovic, *J. Med. Chem.*, 2014, accepted manuscript. DOI: 10.1021/jm501535r
44. M. Lobell, M. Hendrix, B. Hinzen, J. Keldenich, H. Meier, C. Schmeck, R. Schohe-Loop, T. Wunberg and A. Hillisch, *ChemMedChem*, 2006, **1**, 1229–1236.
45. X. Liu, C. Chen and B. J. Smith, *J. Pharmacol. Exp. Ther.*, 2008, **325**, 349–356.
46. P. A. De Oliveira, L. Rotta, A. Pe and J. N. Picada, *Basic Clin. Pharmacol. Toxicol.*, 2006, **99**, 374–378.
47. C.-Y. Cheng, S.-Y. Su, N.-Y. Tang, T.-Y. Ho, S.-Y. Chiang and C.-L. Hsieh, *Brain Res.*, 2008, **1209**, 136–150.
48. S. Gim and P. Koh, *Lab. Anim. Res.*, 2014, **30**, 8–13.
49. F. Blandini, M.-T. Armentero and E. Martignoni, *Parkinsonism Relat. Disord.*, 2008, **14**, S124–S129.
50. M. P. Cunha, M. D. Martín-de-Saavedra, A. Romero, E. Parada, J. Egea, L. Del Barrio, A. L. S. Rodrigues and M. G. López, *Neuroscience*, 2013, **238**, 185–194.
51. X. Lei and J. A. Porco, *J. Am. Chem. Soc.*, 2006, **128**, 14790–14791.
52. R. Bäckström, E. Honkanen, A. Pippuri, P. Kairisalo, J. Pystynen, K. Heinola, E. Nissinen, I. B. Linden, P. T. Männistö and S. Kaakkola, *J. Med. Chem.*, 1989, **32**, 841–846.
53. D. Michelot and M. Meyer, *Nat. Prod. Res.*, 2003, **17**, 41–6.
54. A. Tai, T. Sawano and H. Ito, *Biosci. Biotechnol. Biochem.*, 2014, **76**, 314–318.
55. J.-Y. Feng and Z.-Q. Liu, *J. Agric. Food Chem.*, 2009, **57**, 11041–11046.
56. Y. Yang, Z.-G. Song and Z.-Q. Liu, *Free Radic. Res.*, 2011, **45**, 445–453.
57. C. Y. Huang, R. Zhou, D. C. H. Yang and P. Boon Chock, *Biophys. Chem.*, 2003, **100**, 143–149.
58. R. Scherliess, *Int. J. Pharm.*, 2011, **411**, 98–105.
59. G. Fotakis and J. A. Timbrell, *Toxicol. Lett.*, 2006, **160**, 171–177.
60. A. R. Lupu and T. Popescu, *Toxicol. In Vitro*, 2013, **27**, 1445–1450.

Graphical abstract

